Title	Electrostatic interaction between an enzyme and electrodes in the electric double layer examined in a view of direct electron transfer-type bioelectrocatalysis.
Author(s)	Sugimoto, Yu; Kitazumi, Yuki; Tsujimura, Seiya; Shirai, Osamu; Yamamoto, Masahiro; Kano, Kenji
Citation	Biosensors & bioelectronics (2014), 63: 138-144
Issue Date	2014-07-16
URL	http://hdl.handle.net/2433/189410
Right	© 2014 Elsevier B.V.
Type	Journal Article
Textversion	author

Electrostatic interaction between an enzyme and electrodes in the electric double layer examined in a view of direct electron transfer-type bioelectrocatalysis

Yu Sugimoto,[a] Yuki Kitazumi,[a,b] Seiya Tsujimura,[c] Osamu Shirai,[a] Masahiro Yamamoto,[b,d] Kenji Kano [a,b,*]

a Division of Applied Life Sciences, Graduate School of Agriculture, Kyoto University, Kyoto 606-8502, Japan. E-mail:kano.kenji.5z@kyoto-u.ac.jp, Tel.: +81-75-753-6392; Fax: +81-75-753-6456.

b Japan Science and Technology Agency, CREST, 4-1-8 Honcho, Kawaguchi, Saitama 332-0012, Japan

c Faculty of Pure and Applied Sciences, University of Tsukuba, 1-1-1 Tennodai, Tsukuba, Ibaraki 305-8573, Japan

d Department of Chemistry, Konan University, 8-9-1 Okamoto, Higashi-Nada, Kobe, Hyogo 658-8501, Japan

Abstract

Effects of the electrode potential on the activity of an adsorbed enzyme has been examined by using copper efflux oxidase (CueO) as a model enzyme and by monitoring direct electron transfer (DET)-type bioelectrocatalysis of oxygen reduction. CueO adsorbed on bare Au electrodes at around the point of zero charge (E_{pzc}) shows the highest DET activity, and the activity decreases as the adsorption potential (E_{ad}; at which the enzyme adsorbs) is far from E_{pzc}. We propose a model to explain the phenomena in which the electrostatic interaction between the enzyme and electrodes in the electric double layer affects the orientation and the stability of the adsorbed enzyme. The self-assembled monolayer of butanethiol on Au electrodes decreases the electric field in the outside of the inner Helmholtz plane and drastically diminishes the E_{ad} dependence of the DET activity of CueO. When CueO is adsorbed on bare Au electrodes under open circuit potential and then is held at hold potentials (E_{ho}) more positive than E_{pzc}, the DET activity of the CueO rapidly decreases with the hold time. The strong electric field with positive surface charge density on the metallic electrode (σ_M) leads to fatal denaturation of the

adsorbed CueO. Such denaturation effect is not so serious at $E_{ho} << E_{pzc}$, but the electric field with negative σ_M induces an orientation inconvenient for the DET reaction during the adsorption process. A positively charged neomycin shows a promoter ability to CueO adsorbed at $E_{ad} << E_{pzc}$. The phenomenon is also explained on the proposed model.

Keywords: electric field; electric double layer; direct electron transfer; orientation; denaturation

1. Introduction

Direct electron transfer (DET)-type bioelectrocatalysis of redox enzymes adsorbed on electrodes has gained increasing attention in applications as biosensors and biofuel cells (Armstrong, 2005; Bullen et al., 2006; Reda and Hirst, 2006; Sarma et al., 2009). Although some enzymes show outstanding catalytic performance on suitable electrodes (Cracknell et al., 2008; Kamitaka et al., 2007; Murata et al., 2009; So et al., 2014), detailed mechanism of the electron transfer between enzymes and electrodes remain to be elucidated.

In DET-type bioelectrocatalysis, the distance between the active site of the enzyme and the electrode is the most dominant factor for heterogeneous electron transfer (Chi et al., 2001; Feng et al., 1997; Fujita et al., 2004; Léger and Bertrand, 2008; Niki et al., 2003). In order to shorten the distance, the orientation of enzyme on electrodes is very important. From this viewpoint, several electrode materials have been investigated for DET reaction of proteins. For example, nano-structured materials, such as mesoporous materials, nano-particles and nano-fibers, were used for the study of DET-type bioelectrocatalysis (Baghayeri et al., 2014a, 2014b, 2013; Goldstein et al., 2009; Kamitaka et al., 2007; Murata et al., 2009; Sarma et al., 2009; Tsujimura et al., 2007). When these materials are used as electrodes, the total amounts of the adsorbed enzyme per the projected surface area increase due to an increase in the surface area, and the probability of the orientation convenient for DET reactions seems to increase for enzymes adsorbed in a caged space of mesoporous electrodes.

On the other hand, self-assembled monolayer (SAM)-modified electrodes have been widely used for protein electrochemistry (Allen et al., 1984; Gooding et al., 2001;

Taniguchi et al., 1982; Willner et al., 1997). In recent years, it has been found that surface functional groups drastically affects the DET-type bioelectrocatalytic reaction (Matsumura et al., 2012; Shleev et al., 2006; Tominaga et al., 2008; Tsujimura et al., 2013, 2008a), in which the authors have suggested that the interaction between the specific surface functional groups and enzyme surface leads to an orientation convenient for the DET reaction. Furthermore, since enzymes have some surface charges in solution, charged functional groups will affect the DET activity due to the electrostatic interaction between the enzymes and the SAM-modified electrodes. However, detailed electrostatic interaction has not been clarified.

The object of this study is to elucidate the electrostatic interaction between an enzyme and electrodes in the electric double layer. We assume here that the DET activity is one of measures of the state of the enzyme on the electrode, and we focus on the effect of the adsorption potential (E_{ad}, at which the enzyme adsorbs) and the hold potential (E_{ho}, at which the adsorbed enzyme is held) on the DET-type bioelectrocatalytic current. In this study, we used copper efflux oxidase (CueO) as a model enzyme with DET activity. CueO is one of the multi-copper oxidase (MCO) family that is a very promising catalyst of DET-type bioelectrocatalytic four-electron reduction of O_2 to H_2O (Miura et al., 2007; Tsujimura et al., 2008b). The active site in the MCO contains four copper atoms classified into three types: type I, type II, and type III, according to their spectroscopic properties; the type I copper site is the inlet of electrons from electron-donating substrates or electrodes and transfers the electrons to the trinuclear center composed of one type II copper and two type III copper atoms. The trinuclear center operates as a catalytic site to reduce O_2 to H_2O. CueO has no polysaccharide chains unlike most of the MCOs and the crystal structure of CueO has been determined (PDB code : 1N68). In addition, CueO shows extremely high DET activity (Miura et al., 2007; Tsujimura et al., 2008b). The substrate of the DET reaction is dissolved O_2, and any specific chemicals (which might disturb the electric double layer) are not required to be added in the test solution. Therefore, CueO is suitable as a model enzyme in this study. CueO was adsorbed on a bare Au electrode at various values of E_{ad} and the DET activity was evaluated from the steady-state catalytic current by rotating disc voltammetry. The effect of E_{ho} on the DET activity of the adsorbed CueO was also examined. Based on the results, we will propose a novel model that the surface charge density and the electric field in the electric double

layer affect the enzyme orientation and the stability of CueO on electrodes.

2. Experimental

2.1. Materials

The expression and purification of CueO were carried out as described previously (Miura et al., 2007; Ueki et al., 2006). The coding for the precursor CueO gene was designed to have the *Eco*RI restriction site at the 5'-end and the 6×His-tag coding sequence with *Bam*HI restriction site at 3'-end. The gene was inserted into pUC18, with which *E. coli* BL21 (DE3) was transformed by the heat shock method. The enzyme concentrations were determined using the molar absorption coefficient at 612 nm (ε_{612} = 5800 M^{-1} cm^{-1} (M = mol dm^{-3}) (Ueki et al., 2006)). All chemicals used in this study were of analytical reagent grade, and all solutions were prepared with distilled water.

2.2. Quartz crystal microbalance (QCM) measurement

9-MHz At-cut quartz crystal plates coated with Au were used (Seiko EG&G Co., Ltd), the projected surface area of Au being 0.20 cm^2 and the roughness factor being 1.5 –1.7 (Seiko EG&G: Technical brochure). The Au-coated quartz crystal resonator was attached to a handmade cell with a solution volume of 1 mL (L = dm^3). Measurements were done on a Seiko EG&G QCA922 QCM analyzer with a handmade software for data acquisition.

2.3. Preparation of electrodes

Polycrystalline Au disk electrodes (3-mm diameter) were obtained from BAS, Inc. The Au electrode was polished to a mirror-like finish with Al_2O_3 powder (0.02-μm particle size), rinsed with distilled water, and sonicated in distilled water. Single crystal Au films were prepared on freshly cleaved mica surface (obtained from Nilaco Co.) by vapor deposition (VPC-260, ULVAC KIKO) at less than 1.3×10^{-3} Pa. The temperature of the mica sheet was maintained at 580 °C during the deposition. The Au-deposited mica

sheets were subsequently annealed at 530 °C for 8 h and then quenched in ultrapure water to obtain Au(111) terraces on the sheets (Hobara et al., 1998).

Butanethiol-modified SAM Au(111) electrodes were prepared by immersing the Au-coated mica substrates for at least 24 h in an ethanol solution containing 2 mM butanethiol. Then the electrode was washed with ethanol and ultrapure water before use.

2.4. Electrochemical methods

Almost all electrochemical measurements were performed on a BAS CV 50W, while impedance measurements were performed on an Als704C. Au disk electrodes, Au(111) and butanethiol-modified Au(111) electrodes were used as working electrodes. In rotating disk electrode measurements, the Au disk electrodes were attached to the shaft of an electrode rotator (RDE-1, BAS). Au(111) and butanethiol-modified Au(111) electrodes were attached to the handmade cell with a solution volume of 1.0 mL. The projected surface area of the electrodes is 0.20 cm^2. Electrochemical quartz crystal microbalance (EQCM) measurements were carried out with the Au electrodes for QCM on the QCM resonator as the working electrodes. A Pt wire and an Ag|AgCl|sat. KCl electrode were used as the counter electrode and the reference electrode, respectively. All potentials are referred to the Ag|AgCl|sat. KCl reference electrode in this paper.

Measurements were carried out in pH 5 McIlvaine buffer. The ionic strength was adjusted to be 0.3 M with K_2SO_4. The temperatures of the measurement solution were maintained at 25 ± 1 °C using a water-jacketed cell at a solution volume of 1.0 mL in the rotating disk electrode measurements. Other measurements were carried out at room temperature (25 ± 5 °C).

CueO was adsorbed on the Au disk electrodes as follows unless otherwise stated. An unmodified electrode was immersed into 1.0 mL of McIlvaine buffer in the electrochemical measurement cell. After the working electrode potential was set at E_{ad}, 10 μL of 57 μM CueO solution was injected in the measurement solution, and the solution was stirred for 5 min. Then rotating disk voltammetry was started from an initial potential of 0.6 V without changing the solution.

2.5. Electric double layer capacitance (C_{dl}) calculation

Impedance of real (Z_r) and imaginary (Z_i) parts were recorded on the Als704C.The impedance measurement was performed with A.C. perturbation spectra of sine waves with 10-mV amplitude and frequencies in the range from 0.1 Hz to 1 kHz with 10 steps per decade. The impedance data were analyzed by using a fitting program on Als704C.

3. Results and Discussion

3.1. Effect of the adsorption potential on the DET activity at bare polycrystalline Au electrode

Figure 1A shows steady-state rotating disk voltammograms at CueO-adsorbed polycrystalline Au electrodes in an O_2-saturated buffer, where CueO was adsorbed for 5 min on bare Au electrodes at various adsorption potentials (E_{ad}) except curve (a). Clear reduction currents were observed at CueO-adsorbed electrodes, while no faradaic current appeared at a CueO-unmodified bare Au electrode (curve (a)). Therefore, the current is ascribed to DET-type CueO-catalyzed O_2 reduction (Tsujimura et al., 2008b). The onset potential of the CueO-catalyzed wave was about 0.4 V and was independent of E_{ad}. However, the E_{ad} drastically affected the catalytic current density (I). Figure 1B shows the E_{ad} dependence of the steady-state I value at −0.1 V on the voltammograms. A maximum plateau of I was observed at $E_{ad} \approx 0.4$ V. Furthermore, the I vs. E_{ad} profile showed an asymmetric bell-type curve.

The adsorbed amounts of CueO on the electrode surface were evaluated by EQCM. The E_{ad} value was set at −0.5 V, 0.4 V or 0.8 V in the following experiments. On the addition of a given amount of CueO into the solution, the resonance frequency shift (Δf) decreased with the adsorption time (t_{ad}) due to the adsorption of CueO on the Au electrode and it reached to a limiting value (Δf_{lim}). The Δf_{lim} values and the slope ($d(\Delta f)/dt_{ad}$) were almost independent of E_{ad} examined here. The Δf_{lim} value was 70 ± 20 Hz, which corresponds to a mass density change of 0.4 ±0.1 μg cm^{-2} (Sauerbrey, 1959). Since the molecular mass of CueO is 53.4 kDa (Kim et al., 2001), the mass density change corresponds to a surface concentration (Γ_{QCM}) of $(7 \pm 2) \times 10^{-12}$ mol cm^{-2}. The average

diameter of CueO is assumed to be 6 nm based on the three dimensional information (PDB codes: 1N68) (Roberts et al., 2003, 2002). Then the maximum surface concentration (Γ_{cal}) of CueO is calculated to be 8.0×10^{-12} mol cm^{-2} on a simple model of monolayer packing on a planar electrode with a roughness factor of 1.5. The agreement between Γ_{QCM} and Γ_{cal} suggests that CueO adsorbs on the electrode as a saturated monolayer at all the E_{ad} values examined. In addition, even when the electrode potential was changed from E_{ad} to a hold potential (E_{ho}) after reaching Δf_{lim}, the Δf_{lim} remained practically unchanged, suggesting that no desorption (or further adsorption) occurs on the change from E_{ad} to E_{ho}. Therefore, the E_{ad} dependence of the DET activity cannot be explained in terms of the difference in the adsorption amount of CueO.

Therefore, we consider some electrostatic interactions between CueO and electrodes in the electric double layer. The real and imaginary parts of the impedance at the bare polycrystalline Au electrode were measured and the electric double layer capacitance (C_{dl}) was calculated by analyzing the frequency dependence of the impedance on an equivalent circuit model (Fig. 2A). Figure 2B shows the electrode potential (E) dependence of C_{dl}. Based on Gouy-Chapman theory, in the absence of specific adsorption, the potential of zero charge (E_{pzc}) corresponds to a potential at which

$$\left(\frac{dC_{dl}}{dE}\right)_{E=E_{pzc}} = 0 \qquad (1)$$

Therefore, the data in Fig. 2B indicate that $E_{pzc} \approx 0$ V at C_{dl} of about 20 μF cm^{-2}.

The C_{dl} vs. E plot (Fig. 2B) is similar in shape to the I vs. E_{ad} plot (Fig. 1B). This result suggests that the surface charge is strongly related to the DET activity of the adsorbed CueO. At E_{pzc}, the electric field in the electric double layer formed at the electrode surface is zero. In contrast, at $E_{ad} = -0.5$ V or $E_{ad} = 0.8$ V, the electrode surface charge is large and the electric field becomes strong. This electric field may induce an denaturation of CueO or affect the CueO orientation on the electrode surface. The orientation of CueO would be different between $E_{ad} > E_{pzc}$ and $E_{ad} < E_{pzc}$, since the direction of the electric field is different. Furthermore, since the optimum E_{ad} is slightly more positive than E_{pzc}, weak positive charge on the electrode seems to be convenient for CueO to demonstrate DET-type bioelectrocatalysis (see Fig. S1 (A) as an image).

3.2. Effect of the adsorption potential on the DET activity at bare Au(111) and butanethiol-modified Au(111) electrode

Figure 3 shows the E_{ad} dependence of the I values at −0.1 V of the voltammogram of CueO-catalyzed O_2-reduction at bare Au(111) (panel A) and butanethiol-modified Au(111) electrodes (panel B). Au(111) electrode was used because there is only a limited part of defects of SAM on Au(III) compared with polycrystalline Au. The E_{ad} dependence of the I values at the bare Au(111) electrode is similar to that at the bare polycrystalline Au electrode (Fig. 1B), although the optimum E_{ad} at the bare Au(111) electrode is close to E_{pzc} (of polycrystalline Au) and slightly more negative than that at the bare polycrystalline Au electrode. The difference might be ascribed to the difference in the structure of the electric double layer between polycrystalline and single crystal Au electrode.

On the other hand, the I value at butanethiol-modified Au(111) electrode is almost independent of the E_{ad} (Fig. 3B). The butanethiol-modified Au(111) electrode seems to provide an electric double layer different from that at bare Au electrode.

3.3. Electrostatic interaction between enzyme and electrode

We consider an electrostatic interaction between CueO and electrode in order to explain the phenomena. Figures 4A and 4B show typical interfacial structures on a planer metal electrode and SAM-modified Au electrode, respectively (Ohtani, 1999; Ohtani et al., 1997). The charge density on the electrode surface at $x = 0$ is given by σ_M and ϕ_M is the inner potential of the metallic electrode. The electrode is covered with two dielectric layers of thicknesses of d_1 and d_2 with relative dielectric constants of ε_1 and ε_2, respectively. The diffuse layer ($x > d_1 + d_2$) contains a symmetric z:z electrolyte at a relative dielectric constant of ε_3. The charge density of the inner Helmholtz plane (IHP) at $x = d_1$ is given by σ_{IHP}. The potential at a position x ($\phi(x)$) measured from that of the bulk electrolyte solution ($\phi_S = 0$) is given by Eqs. (2)–(5) (Ohtani, 1999).

$$\phi(x) = \frac{(d_1 - x)\sigma_M}{\varepsilon_1\varepsilon_0} + \frac{d_2(\sigma_M + \sigma_{IHP})}{\varepsilon_2\varepsilon_0} + \phi_F \qquad 0 \le x \le d_1 \tag{2}$$

$$\phi(x) = \frac{(d_1 + d_2 - x)}{\varepsilon_2\varepsilon_0}(\sigma_M + \sigma_{IHP}) + \phi_F \qquad d_1 \le x \le d_1 + d_2 \tag{3}$$

$$\phi(x) = \frac{2RT}{zF}\left|\frac{1 + \tanh\left(\frac{zF\phi_F}{4RT}\right)\exp[\kappa(d_1 + d_2 - x)]}{1 - \tanh\left(\frac{zF\phi_F}{4RT}\right)\exp[\kappa(d_1 + d_2 - x)]}\right| \qquad d_1 + d_2 \le x \tag{4}$$

$$\phi_F = \frac{2RT}{zF}\sinh^{-1}\left[\frac{zF(\sigma_M + \sigma_{IHP})}{2RT\varepsilon_3\varepsilon_0\kappa}\right] \tag{5}$$

where ϕ_F is the potential at the outer Helmholtz plane (OHP, $x = d_1 + d_2$), ε_0 is the dielectric constant in vacuum, κ is inverse of the Debye length, R is the gas constant, T is the absolute temperature, and F is the Faraday constant.

In order to clarify the electric double layer effect, the potential distribution at the electrode/solution interface was calculated. Figure 4C shows the potential distribution at bare Au electrode. In this calculation, specific adsorption of ions on Au electrode was ignored for simplification ($\sigma_{IHP} = 0$). Assuming that H_2O molecules with a diameter of 0.3 nm occupy layer 1 and layer 2, we used $d_1 = 0.15$ nm and $d_2 = 0.3$ nm. The electric field ($d\phi(x)/dx$) in the diffuse layer depends on the applied potential (E) and becomes strong with an increase in $|\sigma_M|$ (or $|E - E_{pzc}|$). The diameter of CueO (about 6 nm) is much larger than the length of the electric double layer (about 1 nm for 100 mM 1:1 electrolyte). However, when CueO adsorbs on the bare Au electrode, the part of the adsorbed CueO facing toward the electrode locates in the electric double layer with strong electric field which depends on σ_M (or $E - E_{pzc}$), because CueO may approach to the inside of IHP. Therefore, the σ_M and the electric field will affect the orientation of CueO adsorption on the electrode. In addition, the charged residues in the part of CueO in the double layer will suffer from strong electrophoretic force at increased $|\sigma_M|$. The isoelectric point of CueO is calculated to be 6.07 on an ExPASy-Compute pI/Mw tool (http://web.expasy.org/compute_pi/). Under the experimental conditions (pH 5), CueO is positively charged as a whole. The positively charged part of the adsorbed CueO will face toward the electrode with $\sigma_M < 0$, and the positively charged residues in the electric double layer will be subjected to a strong attractive force and the negatively charged residues in

the double layer if any will be subjected to a repulsive force at $\sigma_M < 0$. The inverse situation is expected at $\sigma_M > 0$. The force may lead to denaturation of CueO most probably in a cascade mode. These situations seem to result in the E_{ad} dependence of the DET activity at bare Au electrodes.

Since the length of the electric double layer is a function of the ionic strength, we carried out similar experiments on the E_{ad} dependence of the I values at various values of the ionic strength (0.01, 0.005, and 0.001) also (Fig. S2). Although the I value decreased with a decrease in the ionic strength, the I–E_{ad} pattern was almost independent of the ionic strength. Since the ionic strength affects the enzyme activity itself and the solution resistance as well as the electric double layer thickness, the interpretation of the result is not so easy. However, the interpretation described above seems to be effective for the results at such low ionic strength.

On the other hand, the potential distribution at the butanethiol-modified Au electrode is completely different from that at the bare Au electrode, as shown in Fig. 4D. The length of butanethiol SAM (d_1) is 0.7 nm and the surface charge of SAM is zero ($\sigma_{IHP} = 0$). In this case, CueO can approach only to IHP because the SAM occupies inside of IHP. The electric field in the outside of IHP is very weak and is almost independent of $E - E_{pzc}$. This situation seems to be responsible for the fact that the DET activity is almost independent of E_{ad} at the butanethiol-modified Au(111) electrode.

3.4. Effect of the hold potential on adsorbed CueO

We also examined the effect of the hold potential (E_{ho}) on the DET activity of the adsorbed CueO. A bare polycrystalline Au electrode was immersed into the McIlvaine buffer, and an aliquot of the CueO solution (57 μM × 10 μL) was injected into 1.0 mL of the buffer solution under the open circuit potential to adsorb CueO on the Au electrode. After closing the circuit at $t = 0$, rotating disk voltammograms of CueO-catalyzed O_2 reduction were periodically recorded with the electrode. During the interval of the voltammetric measurements, the Au electrode was held at E_{ho} of −0.5 V, 0.4 V, or 0.8 V. Figure 5 shows the relative value of the catalytic current density at a hold time (t_{ho}) against that at $t = 0$ min ($I(t_{ho})/I(0)$) as a function of t_{ho}. The steady-state I values were evaluated

from the rotating disk voltammograms at −0.1 V.

At E_{ho} = 0.4 V, only slight decrease in $I(t_{ho})/I(0)$ was observed. The $I(t_{ho})/I(0)$ maintained 85%-level of the DET-activity even at t_{ho} = 60 min (Fig. 5B). However, at E_{ho} = −0.5 V, $I(t_{ho})/I(0)$ gradually decreased with t_{ho} down to 40% at t_{ho} = 60 min (Fig. 5A).

However, the $I(t_{ho})/I(0)$ value at t_{ho} = 5 min (≈ 87%) is much larger than $I(E_{ad} = -0.5)/I(E_{ad}$ = open circuit potential) (≈ 31%). The latter value was evaluated from Fig. 1B and with an $I(E_{ad}$ = open circuit potential) value of 550 μA cm^{-2}. The difference seems to be ascribed to the difference in the orientation of the adsorbed CueO. The electric field at $\sigma_M < 0$ leads predominantly to an orientation inconvenient for the DET reaction (see Fig. S1 (B) as an image).

On the other hand, the $I(t_{ho})/I(0)$ value rapidly decreased with time at E_{ho} = 0.8 V down to only 5% at t_{ho} = 60 min (Fig. 5C). In contrast to the case at E_{ho} = −0.5 V, the $I(t_{ho})/I(0)$ value at t_{ho} = 5 min (≈ 43%) is close to $I(E_{ad} = -0.5)/I(E_{ad}$ = open circuit potential) (≈ 29%) evaluated from Fig. 1B with the $I(E_{ad}$ = open circuit potential) value. Therefore, the electric field at $\sigma_M > 0$ leads predominantly to denaturation of the adsorbed CueO triggered by the exposure of the facing part of CueO in the strong electric field. The asymmetric behavior of I vs. E_{ad} in Fig. 1B seems to be ascribed to the difference in the contribution of the orientation effect and the denaturation effect between the positive and negative sides of σ_M.

In order to verify the denaturation of CueO on the electrode at positive σ_M, cyclic voltammetric measurements were performed in the buffer solution containing 1 mM $K_4[Fe(CN)_6]$ by using CueO-adsorbed Au electrodes. CueO-adsorbed Au electrode surface can be indirectly characterized by the electrode reaction of $[Fe(CN)_6]^{3-/4-}$ as a pilot (or marker) redox couple. When a CueO-adsorbed electrode at t_{ho} = 0 min was used, clear redox peaks of $[Fe(CN)_6]^{3-/4-}$ was observed (Fig. 5C, inset curve (a)). This indicates that $[Fe(CN)_6]^{3-/4-}$ can diffuse onto and from the electrode surface through the gaps among the native CueO of the adsorbed monolayer. At E_{ho} = −0.5 V and 0.4 V (at various t_{ho}), the shape of the cyclic voltammograms of $[Fe(CN)_6]^{3-/4-}$ were almost identical with that observed at t_{ho} = 0 min (data not shown). This result supports the idea that the electric field at E = −0.5 V mainly leads to the orientation inconvenient for the DET-type bioelectrocatalytic reaction.

In contrast, at E_{ho} = 0.8 V, the peak current density of $[Fe(CN)_6]^{3-/4-}$ decreased

and the peak was broadened with an increase in t_{ho} (Fig. 5C inset). This result suggests that CueO is denatured at E = 0.8 V and the denatured CueO covers the Au electrode surface to hinder the diffusion and the electron transfer kinetics of $[Fe(CN)_6]^{3-/4-}$.

3.5. Protection of CueO from the electric field by a promoter

As discussed in the previous sections, the strong electric field affects the orientation and the stability of the adsorbed CueO. We expect that some compounds as additives can minimize such inconvenient effects of the electric field effect against CueO, as in the case of butanethiol-SAM. Neomycin is a positively charged molecule and is often used as a promoter for DET reactions (Heering and Hagen, 1996; Johnson et al., 2002). Promoters do not directly involved in the electron transfer, but facilitate DET reactions. This phenomenon has been explained in terms of the promoter-assisted enzyme adsorption on electrodes and/or the electrostatic interaction between enzymes and promoters (Allen et al., 1984; Eddowes and Hill, 1979). In this work, effect of neomycin on the DET-type bioelectrocatalysis of CueO was examined at various values of E_{ad}.

Bare polycrystalline Au electrodes were immersed into the McIlvaine buffer, and aliquots of CueO solution and neomycin solution were separately injected into the buffer solution at a given E_{ad} for 5 min under stirring to adsorb CueO on the Au electrode surface. The steady-state I values at −0.1 V were evaluated from the rotating disk voltammograms of CueO-catalyzed O_2 reduction. The I values at various concentrations of neomycin and at three different E_{ad} are depicted in Fig. 6.

At E_{ad} = 0.4 V and 0.8 V, the I values were almost independent of the neomycin concentration. Since positively charged neomycin is difficult to approach to the electrode surface at $E_{ad} > E_{pzc}$ due to the electrostatic repulsion, the electric field effect on CueO is not affected by neomycin. On the other hand, the drastic effect of the neomycin addition on the I value was observed at E_{ad} = −0.5 V; the I value increased with an increase in the logarithmic value of the neomycin concentration and was identical with that at E_{ad} = 0.4 V in the neomycin concentration of 0.1% (wt/vol). At E = −0.5 V, positively charged neomycin adsorbs on the Au electrode surface more rapidly than CueO by the attractive electrostatic interaction. The increase in the I value with the addition of neomycin suggests that this neomycin layer provide a surface situation close to that at E_{ad} = 0.4 V.

Fortunately, the electrostatic interaction between CueO and neomycin does not seem to cause serious denaturation effect as such observed in the positive σ_M side (i. e. E = 0.8 V).

4. Conclusion

It has been found that the DET-type bioelectrocatalytic reaction of CueO is strongly affected by both of the adsorption and the hold potentials (E_{ad} and E_{ho}) at bare Au electrodes. Based on the fact that the E_{ad} and E_{ho} do not affect the total surface concentration of the adsorbed CueO and that the SAM formation of butanethiol on Au electrode drastically diminishes E_{ad} dependence of the DET-activity of CueO, we have proposed that the electrostatic interaction of CueO in the electric double layer affects the orientation and the stability of the adsorbed CueO. The interaction in the electric double layer formed with negative σ_M seems to lead to an orientation inconvenient for the DET reaction of CueO, but does not lead to fatal denaturation of CueO. On the other hand, weak positive charge on the electrode seems to be convenient for CueO to demonstrate DET-type bioelectrocatalysis, but strong interaction of CueO in the electric double layer with large positive σ_M causes fatal denaturation of CueO. It has been also found that a positively charged neomycin is effective to minimize the negative effect by the electric double layer formed with negative σ_M. The phenomena can be explained with the model proposed here. Since the interaction will depend on each individual enzyme and each electrode, the effect of the electric double layer on the enzyme activity will also depend on enzyme and electrode used. Further investigation is required to strength our proposed model. However, the concept proposed here would become important for developing DET-type bio-devices such as biosensors or biofuel cells in future.

Acknowledgement

This work was supported in part by Japan Science and Technology Agency, CREST (to MY).

References

Allen, P., Allen, H., Hill, O., Walton, N., 1984. Surface modifiers for the promotion of direct electrochemistry of cytochrome *c*. J. Electroanal. Chem. Interfacial Electrochem. 178, 69–86.

Armstrong, F.A., 2005. Recent developments in dynamic electrochemical studies of adsorbed enzymes and their active sites. Curr. Opin. Chem. Biol. 9, 110–117.

Baghayeri, M., Nazarzadeh, E., Hasanzadeh, R., 2014a. Facile synthesis of PSMA-g - 3ABA/MWCNTs nanocomposite as a substrate for hemoglobin immobilization : Application to catalysis of H_2O_2. Mater. Sci. Eng. C 39, 213–220.

Baghayeri, M., Nazarzadeh, E., Mansour, M., 2014b. A simple hydrogen peroxide biosensor based on a novel electro-magnetic poly (p -phenylenediamine)@ Fe_3O_4 nanocomposite. Biosens. Bioelectron. 55, 259–265.

Baghayeri, M., Nazarzadeh, E., Namadchian, M., 2013. Direct electrochemistry and electrocatalysis of hemoglobin immobilized on biocompatible poly (styrene-alternative-maleic acid)/ functionalized multi-wall carbon nanotubes blends. Sensors Actuators B. Chem. 188, 227–234.

Bullen, R.A., Arnot, T.C., Lakeman, J.B., Walsh, F.C., 2006. Biofuel cells and their development. Biosens. Bioelectron. 21, 2015–2045.

Chi, Q., Zhang, J., Andersen, J.E.T., Ulstrup, J., 2001. Ordered Assembly and Controlled Electron Transfer of the Blue Copper Protein Azurin at Gold(111) Single-Crystal Substrates. J. Phys. Chem. B 105, 4669–4679.

Cracknell, J., Vincent, K., Armstrong, F., 2008. Enzymes as working or inspirational electrocatalysts for fuel cells and electrolysis. Chem. Rev. 108, 2439–2461.

Eddowes, M.J., Hill, H.A., 1979. Electrochemistry of Horse Heart Cytochrome *c*. J. Am. Chem. Soc. 101, 4461–4464.

Feng, Z.Q., Imabayashi, S., Kakiuchi, T., Niki, K., 1997. Long-range electron-transfer reaction rates to cytochrome c across long-and short-chain alkanethiol self-assembled monolayers: Electroreflectance studies. J. Chem. Soc. Faraday Trans. 1367–1370.

Fujita, K., Nakamura, N., Ohno, H., Leigh, B.S., Niki, K., Gray, H.B., Richards, J.H., 2004. Mimicking Protein-Protein Electron Transfer : Voltammetry of *Pseudomonas aeruginosa* Azurin and the *Thermus thermophilus* CuA Domain at ω-Derivatized Self-Assembled-MOnolayer gold Electrodes. J. Am. Chem. Soc. 126, 13954–13961.

Goldstein, D.C., Thordarson, A.P., A, J.R.P., 2009. The Bioconjugation of Redox Proteins to Novel Electrode Materials. Aust. J. Chem. 62, 1320–1327.

Gooding, J.J., Erokhin, P., Losic, D., Yang, W., Policarpio, V., Liu, J., Ho, F.M., Situmorang, M., Hibbert, D.B., Shapter, J.G., 2001. Parameters important in fabricating enzyme electrodes using self-assembled monolayers of alkanethiols. Anal. Sci. 17, 3–9.

Heering, H.A., Hagen, W.R., 1996. Complex electrochemistry of flavodoxin at carbon-based electrodes: results from a combination of direct electron transfer, flavin-mediated electron transfer and comproportionation. J. Electroanal. Chem. 404, 249–260.

Hobara, D., Ota, M., Imabayashi, S., Niki, K., Kakiuchi, T., 1998. Phase separation of binary self-assembled thiol monolayers composed of 1-hexadecanethiol and 3-mercaptopropionic acid on Au(111) studied by scanning tunneling microscopy and cyclic voltammetry. J. Electroanal. Chem. 444, 113–119.

Johnson, D.L., Maxwell, C.J., Losic, D., Shapter, J.G., Martin, L.L., 2002. The influence of promoter and of electrode material on the cyclic voltammetry of *Pisum sativum* plastocyanin. Bioelectrochemistry 58, 137–147.

Kamitaka, Y., Tsujimura, S., Setoyama, N., Kajino, T., Kano, K., 2007. Fructose/dioxygen biofuel cell based on direct electron transfer-type bioelectrocatalysis. Phys. Chem. Chem. Phys. 9, 1793–1801.

Kim, C., Lorenz, W.W.L., HOOPES, J.T., DEAN, J.F.D., 2001. Oxidation of phenolate siderophores by the multicopper oxidase encoded by the *Escherichia coli yacK* gene. J. Bacteriol. 183, 4866–4875.

Léger, C., Bertrand, P., 2008. Direct electrochemistry of redox enzymes as a tool for mechanistic studies. Chem. Rev. 108, 2379–2438.

Matsumura, H., Ortiz, R., Ludwig, R., 2012. Direct electrochemistry of *Phanerochaete chrysosporium* cellobiose dehydrogenase covalently attached onto gold nanoparticle modified solid gold electrodes. Langmuir 28, 10925–10933.

Miura, Y., Tsujimura, S., Kamitaka, Y., Kurose, S., Kataoka, K., Sakurai, T., Kano, K., 2007. Bioelectrocatalytic reduction of O_2 catalyzed by CueO from *Escherichia coli* adsorbed on a highly oriented pyrolytic graphite electrode. Chem. Lett. 36, 132–133.

Murata, K., Kajiya, K., Nakamura, N., Ohno, Hi., 2009. Direct electrochemistry of bilirubin oxidase on three-dimensional gold nanoparticle electrodes and its application in a biofuel cell. Energy Environmenatalmenatal Sci. 2, 1280–1285.

Niki, K., Hardy, W.R., Hill, M.G., Li, H., Sprinkle, J.R., Margoliash, E., Fujita, K., Tanimura, R., Nakamura, N., Ohno, H., Richards, J.H., Gray, H.B., 2003. Coupling to Lysine-13 Promotes Electron Tunneling through Carboxylate-Terminated Alkanethiol Self-Assembled Monolayers to Cytochrome *c*. J. Phys. Chem. B 107, 9947–9949.

Ohtani, M., 1999. Quasi-reversible voltammetric response of electrodes coated with electroactive monolayer films. Electrochem. commun. 1, 488–492.

Ohtani, M., Kuwabata, S., Yoneyama, H., 1997. Voltammetric response accompanied by inclusion of ion pairs and triple ion formation of electrodes coated with an electroactive monolayer film. Anal. Chem. 69, 1045–1053.

Reda, T., Hirst, J., 2006. Interpreting the catalytic voltammetry of an adsorbed enzyme by considering substrate mass transfer, enzyme turnover, and interfacial electron transport. J. Phys. Chem. B 110, 1394–1404.

Roberts, S. a, Wildner, G.F., Grass, G., Weichsel, A., Ambrus, A., Rensing, C., Montfort, W.R., 2003. A labile regulatory copper ion lies near the T1 copper site in the multicopper oxidase CueO. J. Biol. Chem. 278, 31958–31963.

Roberts, S.A., Weichsel, A., Grass, G., Thakali, K., Hazzard, J.T., Tollin, G., Rensing, C., Montfort, W.R., 2002. Crystal structure and electron transfer kinetics of CueO, a multicopper oxidase required for copper homeostasis in *Escherichia coli*. Proc. Natl. Acad. Sci. U. S. A. 99, 2766–2771.

Sarma, A.K., Vatsyayan, P., Goswami, P., Minteer, S.D., 2009. Recent advances in material science for developing enzyme electrodes. Biosens. Bioelectron. 24, 2313–2322.

Sauerbrey, G.Z., 1959. Verwendung von Schwingquarzen zur Wägung dünner Schichten und zur Mikrowägung. Zeitschrift für Phys. A Hadron. Nucl. 155, 206–222.

Shleev, S., Pita, M., Yaropolov, A.I., Ruzgas, T., Gorton, L., 2006. Direct Heterogeneous Electron Transfer Reactions of *Trametes hirsuta* Laccase at Bare and Thiol-Modified Gold Electrodes. Electroanalysis 18, 1901–1908.

So, K., Kawai, S., Hamano, Y., Kitazumi, Y., Shirai, O., Hibi, M., Ogawa, J., Kano, K., 2014. Improvement of a direct electron transfer-type fructose/dioxygen biofuel cell with a substrate-modified biocathode. Phys. Chem. Chem. Phys. 16, 4823–4829.

Taniguchi, I., Toyosawa, K., Yamaguchi, H., Yasukouchi, K., 1982. Voltammetric response of horse heart cytochrome c at a gold electrode in the presence of sulfur bridged bipyridines. J. Electroanal. Chem. 140, 187–193.

Tominaga, M., Ohtani, M., Taniguchi, I., 2008. Gold single-crystal electrode surface modified with self-assembled monolayers for electron tunneling with bilirubin oxidase. Phys. Chem. Chem. Phys. 10, 6928–6934.

Tsujimura, S., Abo, T., Matsushita, K., Ano, Y., Kano, K., 2008a. Direct Electron Transfer Reaction of D-Gluconate 2-Dehydrogenase Adsorbed on Bare and Thiol-modified Gold Electrodes. Electrochem. commun. 76, 549–551.

Tsujimura, S., Asahi, M., Goda-Tsutsumi, M., Shirai, O., Kano, K., Miyazaki, K., 2013. Direct electron transfer to a metagenome-derived laccase fused to affinity tags near the electroactive copper site. Phys. Chem. Chem. Phys. 15, 20585–20589.

Tsujimura, S., Kamitaka, Y., Kano, K., 2007. Diffusion-Controlled Oxygen Reduction on Multi-Copper Oxidase-Adsorbed Carbon Aerogel Electrodes without Mediator. Fuel Cells 6, 463–469.

Tsujimura, S., Miura, Y., Kano, K., 2008b. CueO-immobilized porous carbon electrode exhibiting improved performance of electrochemical reduction of dioxygen to water. Electrochim. Acta 53, 5716–5720.

Ueki, Y., Inoue, M., Kurose, S., Kataoka, K., Sakurai, T., 2006. Mutations at Asp112 adjacent to the trinuclear Cu center in CueO as the proton donor in the four-electron reduction of dioxygen. FEBS Lett. 580, 4069–4072.

Willner, I., Katz, E., Willner, B., 1997. Assembly of functionalized monolayers of redox proteins on electrode surfaces: novel bioelectronic and optobioelectronic systems. Biosens. Bioelectron. 12, 337–356.

Figure Legends

Fig. 1. (A) Steady-state rotating disk voltammograms in an O_2-saturate buffer (pH 5.0) at (a) CueO-unmodified bare Au electrode and (b–h) CueO-adsorbed polycrystalline Au electrodes at E_{ad} = (b) −0.5 V, (c) −0.2 V, (d) 0 V, (e) 0.2 V, (f) 0.4 V, (g) 0.6 V and (h) 0.8 V. The voltammograms were recorded at 2000 rpm, 25 °C and at a scan rate of 20 mV s^{-1}. (B) E_{ad} dependence of the I value at −0.1 V of the voltammogram. The points represent average values of 3-4 measurements with another electrode, and the error bars were evaluated by the Student t-distribution at 90% confidence level.

Fig. 2. (A) The equivalent circuit model used to obtain the double layer capacitance. C_{dl} is the electric double layer capacitance, R_{ct} is the charge transfer resistance, and R_{Ω} is the solution resistance.
(B) Electrode potential dependence of C_{dl}. The impedance measurements were done under Ar-atmosphere to avoid faradic contribution and at 25 °C. The error bars were evaluated by the Student t-distribution at 90% confidence level.

Fig. 3. E_{ad} dependence of the I value at −0.1 V of voltammogram of CueO-catalyzed O_2-reduction at (A) bare Au(111) and (B) butanethiol-modified Au(111) electrode. The cyclic

voltammetry was done under the O_2 saturated conditions at room temperature and at a scan rate of 20 mV s^{-1}. The error bars were evaluated by the Student *t*-distribution at 90% confidence level.

Fig. 4. Typical interfacial structures on (A) planer metal and (B) SAM-modified Au electrodes. Calculated potential distributions of (C) bare Au and (D) butanethiol-modified Au electrode. $E - E_{pzc}$ = (a) +0.6 V, (b) +0.4 V, (c) +0.2 V, (d) 0 V, (e) −0.2 V, (f) −0.4 V, (g) −0.6 V. The parameters used in calculation: (C) d_1 = 0.15 nm, d_2 = 0.3 nm, ε_1 = 78.5, ε_2 = 78.5, ε_3 = 78.5, σ_{IHP} = 0 C m^{-2}, T = 298 K, z = 1; (D) d_1 = 0.7 nm, d_2 = 0.15 nm, ε_1 = 3, ε_2 = 78.5, ε_3 = 78.5, σ_{IHP} = 0 C m^{-2}, T = 298 K, z = 1.

Fig. 5. The relative value of the catalytic current density as a function of t_{ho} at E_{ho} = (A) −0.5 V, (B) 0.4 V, and (C) 0.8 V. The rotating disk voltammograms were recorded under O_2-saturated conditions at a rotating rate of 2000 rpm, 25 °C and at a scan rate of 20 mV s^{-1}. The inset is cyclic voltammograms in the buffer solution containing 1mM $K_4[Fe(CN)_6]$ using CueO-adsorbed Au electrode at t_{ho} (at E_{ho} = 0.8 V) = (a) 0 min, (b) 10 min, (c) 20 min, (d) 40 min, and (e) 60 min. The cyclic voltammograms were recorded at 25 ˚C and at a scan rate of 20 mV s^{-1}.

Fig. 6. Comparison of the I values at various concentrations of Neomycin and at E_{ad} = (a) −0.5 V, (b) 0.4 V, and (c) 0.8 V. The cyclic voltammograms were recorded under O_2-saturated conditions at a rotating rate of 2000 rpm, 25 °C and at a scan rate of 20 mV s^{-1}.

(A)

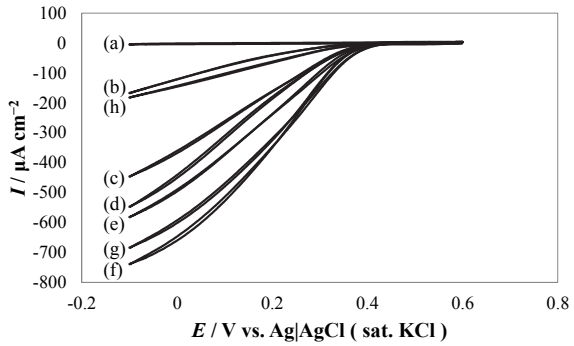

(B)

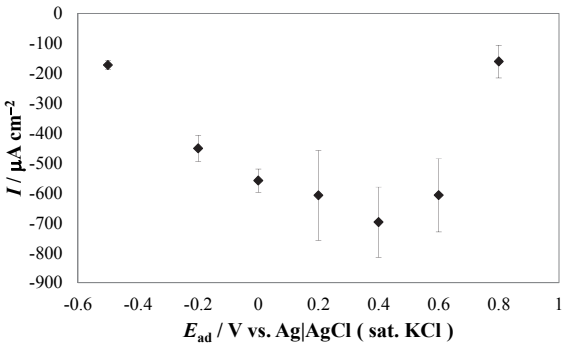

Fig. 1

(A)

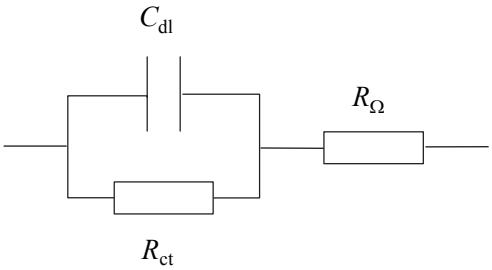

(B)

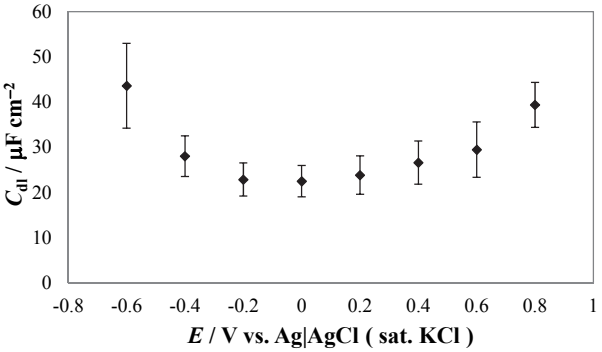

Fig. 2

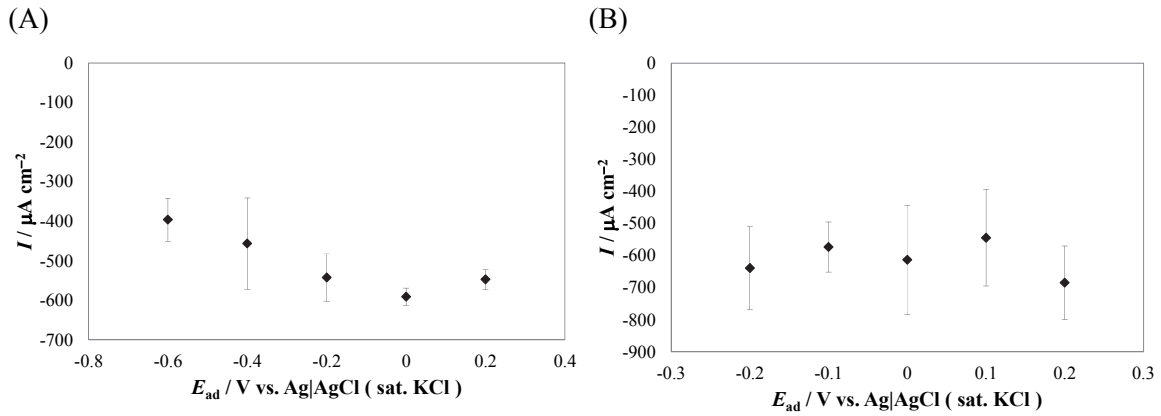
(A)
(B)
0
-100
-200
-300
-400
-500
-600
-700
-800
-900
I / μA cm−2
-0.8
-0.6
-0.4
-0.2
0
0.2
0.4
-0.3
-0.1
0.1
0.3
Ead / V vs. Ag|AgCl (sat. KCl)

Fig. 3

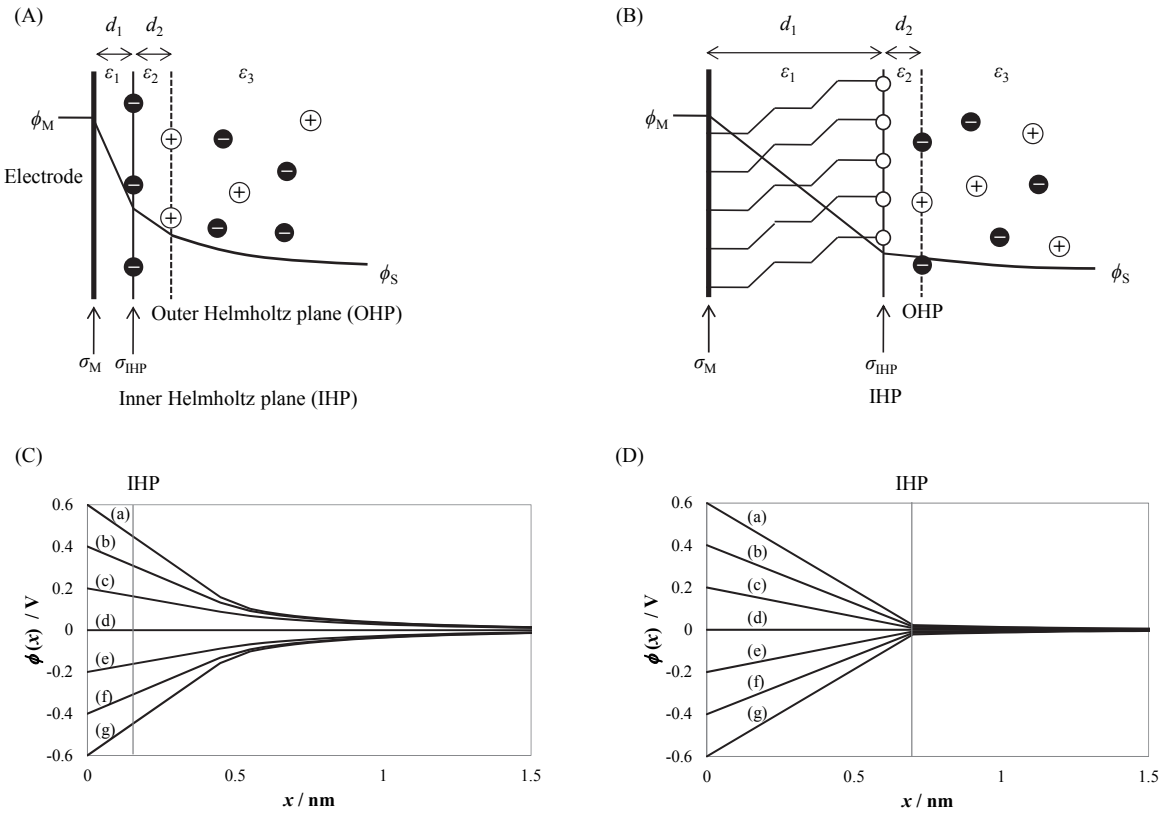
(A)
(B)
d1
d2
ε1
ε2
ε3
ϕM
ϕS
Electrode
Outer Helmholtz plane (OHP)
σM
σIHP
Inner Helmholtz plane (IHP)
OHP
IHP
(C)
(D)
(a)
(b)
(c)
(d)
(e)
(f)
(g)
ϕ (x) / V
x / nm
0.6
0.4
0.2
0
-0.2
-0.4
-0.6
0
0.5
1
1.5

Fig. 4

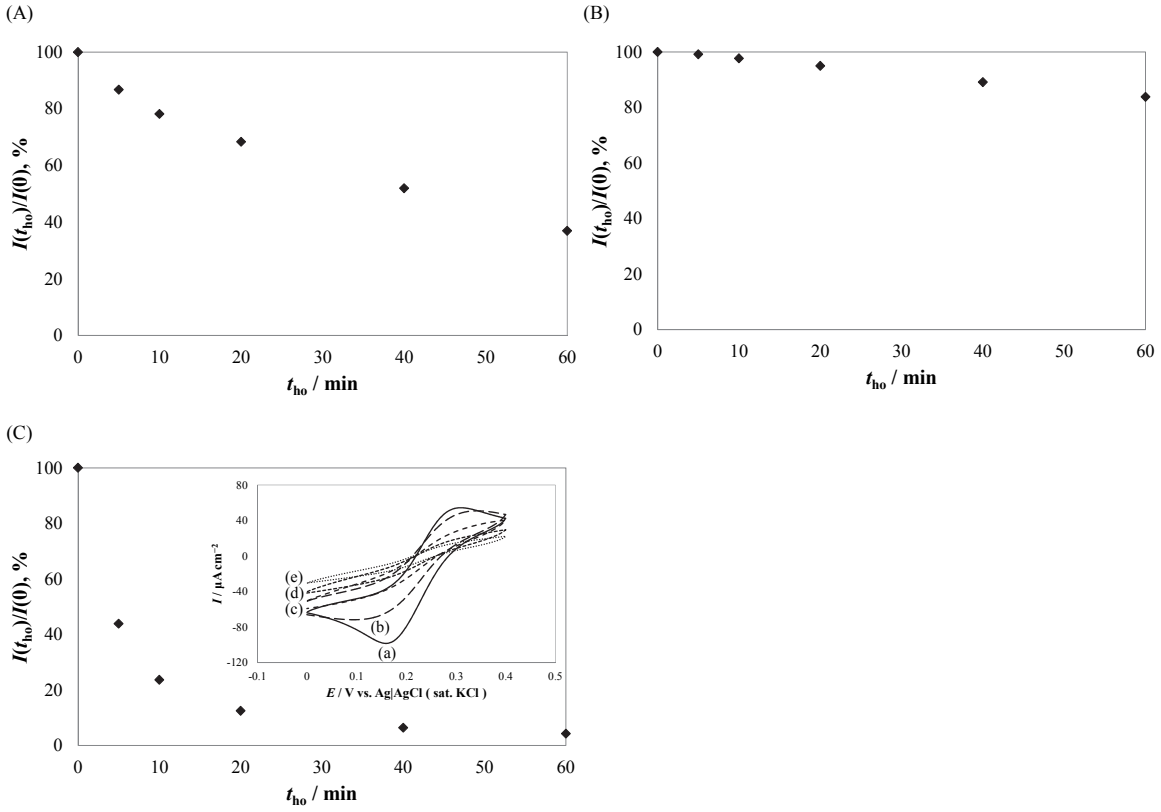
(A)
(B)
(C)
$I(t_{ho})/I(0)$, %
t_{ho} / min
I / μA cm^{-2}
E / V vs. Ag|AgCl (sat. KCl)
(a)
(b)
(c)
(d)
(e)

Fig. 5

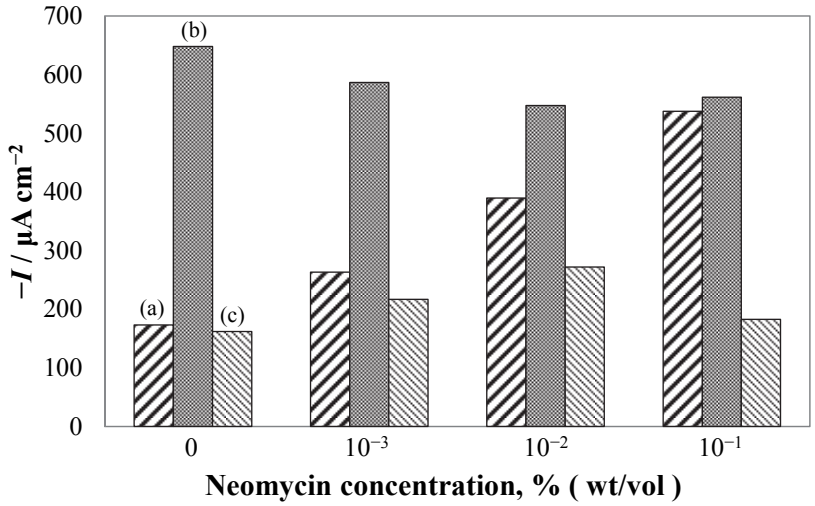
$-I$ / μA cm^{-2}
Neomycin concentration, % (wt/vol)
(a)
(b)
(c)
0
10^{-3}
10^{-2}
10^{-1}

Fig. 6

Electrostatic interaction between an enzyme and electrodes in the electric double layer examined in a view of direct electron transfer-type bioelectrocatalysis

Yu Sugimoto,[a] Yuki Kitazumi,[a,b] Seiya Tsujimura,[c] Osamu Shirai,[a] Masahiro Yamamoto,[b,d] Kenji Kano [a,b,*]

a Division of Applied Life Sciences, Graduate School of Agriculture, Kyoto University, Kyoto 606-8502, Japan. E-mail:kano.kenji.5z@kyoto-u.ac.jp, Tel.: +81-75-753-6392; Fax: +81-75-753-6456.

b Japan Science and Technology Agency, CREST, 4-1-8 Honcho, Kawaguchi, Saitama 332-0012, Japan

c Faculty of Pure and Applied Sciences, University of Tsukuba, 1-1-1 Tennodai, Tsukuba, Ibaraki 305-8573, Japan

d Department of Chemistry, Konan University, 8-9-1 Okamoto, Higashi-Nada, Kobe, Hyogo 658-8501, Japan

Supplementary Information

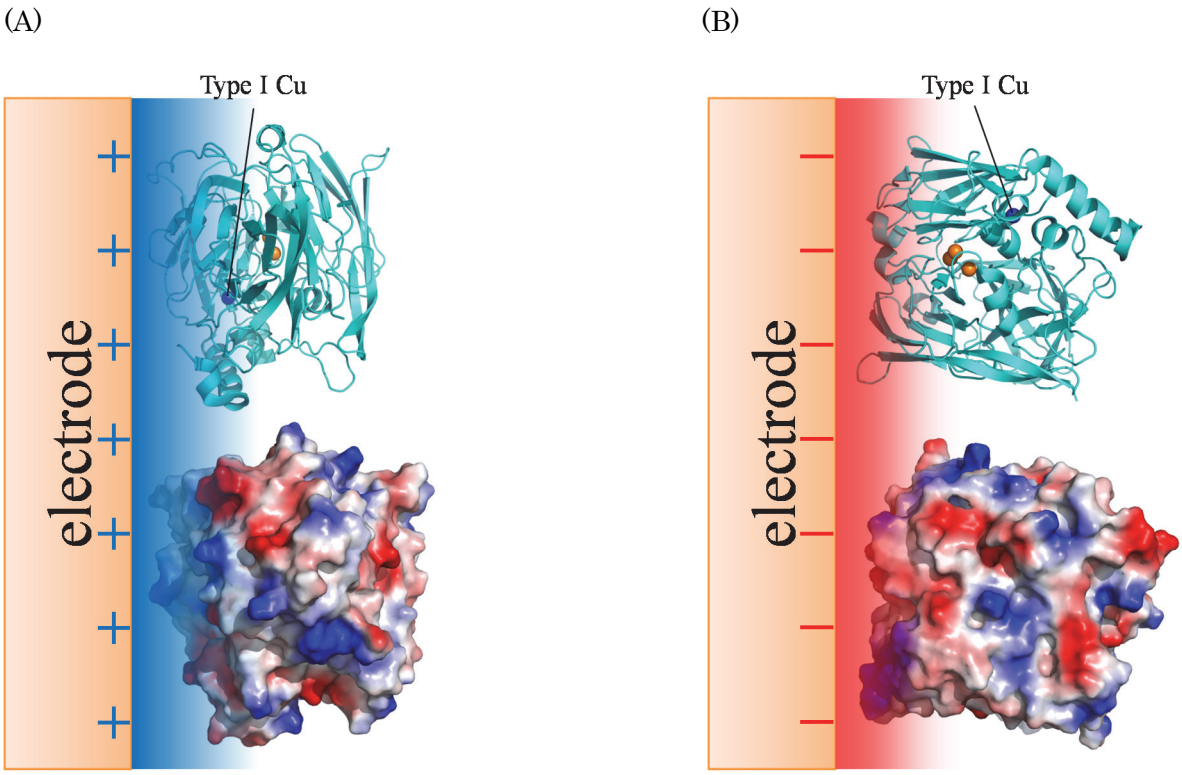

Fig. S1. The image cartoon of the orientation of adsorbed CueO at (A) $\sigma_M > 0$ and (B) $\sigma_M < 0$.

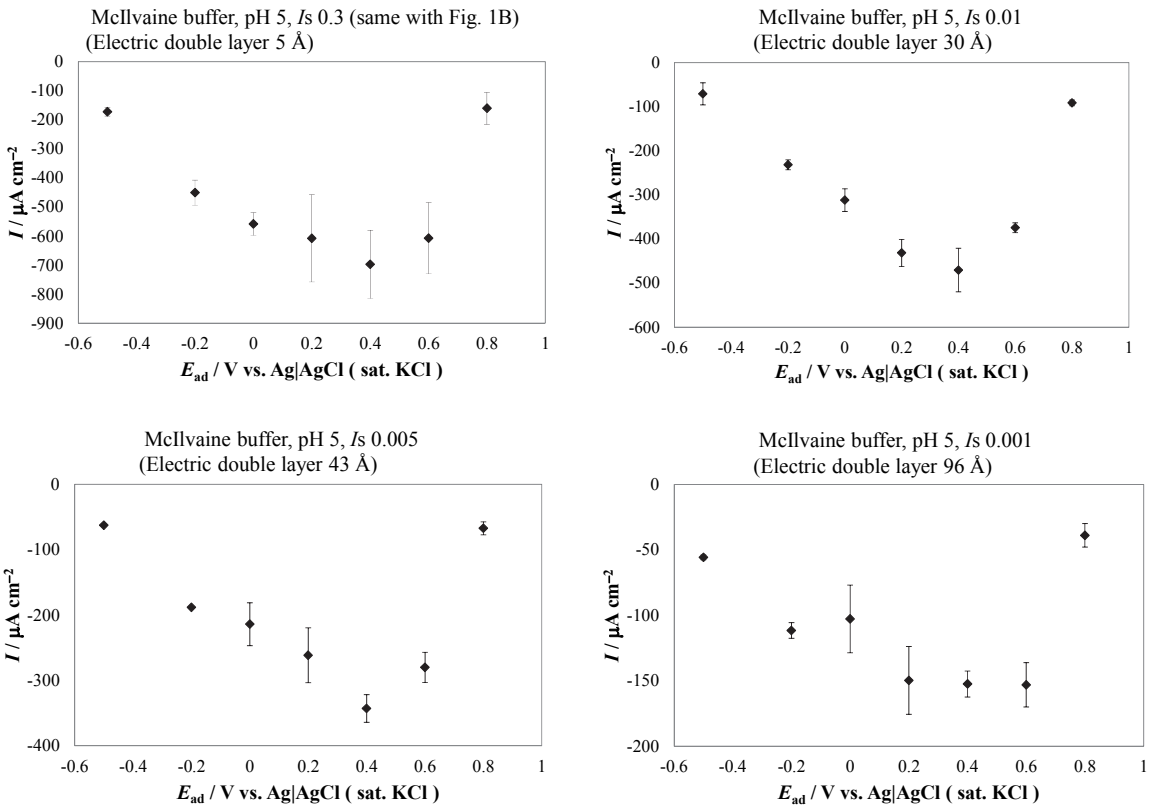

Fig. S2. E_{ad} dependence of the I value at −0.1 V of the voltammogram at various values of the ionic strength (I_s). The points represent average values of 3-4 measurements with independent electrodes, and the error bars were evaluated by the Student t-distribution at 90% confidence level. The voltammograms were recorded at 2000 rpm and 25 °C.